We are IntechOpen,
the world's leading publisher of
Open Access books
Built by scientists, for scientists

6,900
Open access books available

186,000
International authors and editors

200M
Downloads

Our authors are among the

154
Countries delivered to

TOP 1%
most cited scientists

12.2%
Contributors from top 500 universities

CLARIVATE ANALYTICS

BOOK CITATION INDEX

INDEXED

WEB OF SCIENCE™

Selection of our books indexed in the Book Citation Index
in Web of Science™ Core Collection (BKCI)

Interested in publishing with us?
Contact book.department@intechopen.com

DFT-based Theoretical Simulations for Photocatalytic Applications Using TiO$_2$

Yeliz Gurdal and Marcella Iannuzzi

Abstract

TiO$_2$ has been shown to be a potential candidate for photoinitiated processes, such as dye sensitized solar cells and water splitting in production of H$_2$. The large band gap of TiO$_2$ can be reduced by functionalizing the oxide by adsorbing dye molecules and/or water reduction/oxidation catalysts, by metal/nonmetal doping, and by mixing with another oxide. Due to these methods, several different TiO$_2$-based complexes can be constructed having different geometries, electronic structures, and optical characteristics. It is practically impossible to test the photocatalytic activity of all possible TiO$_2$-based complexes using only experimental techniques. Instead, density functional theory (DFT)-based theoretical simulations can easily guide experimental studies by screening materials and providing insights into the photoactivity of the complexes. The aim of this chapter is to provide an outlook for current research on DFT-based simulations of TiO$_2$ complexes for dye sensitized solar cells and water splitting applications and to address challenges of theoretical simulations.

Keywords: density functional theory, ab-initio molecular dynamics, photocatalyst, TiO$_2$, dye sensitized solar cells, water splitting

1. Introduction

Emergent technologies and the demand for alternative energy sources, which do not produce greenhouse gases as a byproduct lead to a growing awareness in using those renewable sources already provided by nature, such as sunlight. The ideal goal is to emulate the photochemical process with which the plants convert H$_2$O and CO$_2$ into O$_2$ and carbohydrates by absorbing photons in the energy range between 3.3 and 1.5 eV (visible spectrum). Scientists then aim at designing new catalysts that can employ the easily available sunlight and convert it into chemical energy, without depending on the activation energy generated by traditional fuels.

In 1938, for the first time, Goodeve and Kitchener [1] demonstrated the photocatalytic activity of the TiO$_2$ surface, which can produce oxygen by absorbing UV light thus leading to the photobleaching of dyes. This study has initiated many others toward discovering photocatalytic reactions that can be catalyzed by TiO$_2$. The success of this material is also justified by its high stability, low cost, no side effects on humans and environment, and ease in large-scale usage. In spite of the promising properties of TiO$_2$, the photocatalytic activity of the bare surface is not optimal, due to the too large energy gap [2]. This limits the photons' absorption and induces the fast recombination of the photogenerated carriers [3]. While these drawbacks significantly hinder the effective application of the pristine material, several possible solutions have been envisioned by considering surface modifications, such as composite semiconductor coupling, metal/nonmetal doping, and functionalization by means of different types of adsorbates [4]. For instance, Zn-porphyrin adsorbed on the TiO$_2$ surface reduces the threshold for the photons' absorption, and by allowing the fast electron injection toward the substrate, slows down the charge recombination process [5].

Among many photocatalytic applications of functionalized TiO$_2$ surface, water splitting for H$_2$ production and dye sensitized solar cells (DSSCs) are among the most widely studied topics. Although the increasing number of promising studies is going to build photocatalytically efficient and robust several TiO$_2$-based materials, in this field, the support of the theoretical approach to explore the properties of possible candidate materials is essential. The investigation of proper atomistic models of the systems of interest, possibly including the electronic structure characterization and reproducing the relevant processes, can significantly help the screening of materials. In particular, it is necessary to understand the nature of the adsorbate-substrate interaction, and providing insights into the photoactivity prior to extensive experimental efforts. The aim of this chapter is to review the current progress and challenges in density functional theory (DFT)-based simulations of functionalized TiO$_2$ surfaces, including rutile, anatase, and TiO$_2$ nanoparticles, with respect to the applications in photocatalytic water splitting and DSSCs.

2. Overview on density functional theory

DFT is developed by Hohenberg, Kohn, and Sham [6, 7] in 1964 as a minimization problem of the ground state energy as a function of electron density. The approach is to solve any fully interacting problem by mapping it to a noninteracting problem introducing exchange-correlation functional, see Eq. (1).

$$E = T_s[\rho(r)] + J[\rho(r)] + \int v_{ext}(r)\,\rho(r)\,dr + E_{xc}[\rho(r)] \tag{1}$$

where $T_s[\rho(r)]$ is the kinetic energy of the noninteracting system, $J[\rho(r)]$ is the classical Coulomb repulsion energy, $\int v_{ext}(r)\,\rho(r)\,dr$ is the interaction of the external potential acting on the electrons, and $E_{xc}[\rho(r)]$ term is the exchange and correlational energy. All of these terms are called functionals and they depend on the electron density $\rho(r)$, i.e., the number of electrons per unit volume.

Electron density can be expressed in many ways [8]; however, Gaussian and plane wave formalism is shown to be significantly efficient for the description of the orbitals [9]. A localized Gaussian basis set positioned at each atom is used to expand the Kohn-Sham orbitals and an auxiliary plane wave basis set is used to describe the electron density, thus improving the computational performance in the calculation of the Coulomb interactions. This scheme is shown to be a suitable choice for large-scale DFT simulations [10, 11].

Although the achievement in introducing electron density depends on the total energy instead of the electron wave function formalism and providing simple, universal, and self-consistent-field description of the ground-state electronic structure, any practical usage of DFT requires an accurate description to the exchange and correlational effects, $E_{xc}[\rho(r)]$, see Eq. (2).

$$E_{xc}[\rho(r)] = (V_{ee}[\rho(r)] - J[\rho(r)]) + (T[\rho(r)] - T_s[\rho(r)]) \tag{2}$$

where $T[\rho(r)]$ is the kinetic energy of the interacting system and $V[\rho(r)]$ is the nonclassical interaction between electrons. Although the exact analytic expression of the exchange-correlation functional is not known, approximations to these terms have been demonstrated to be able capture most of the physical/chemical properties of many systems from the solid state to the liquid state.

Many methods have been proposed to calculate exchange-correlation contribution to the total energy [12]. One of the most commonly used ones is the generalized gradient approximation (GGA), where the exchange and correlation energy depends on both electron density and its gradient [13]. This method includes semiempirical functionals that consist of one or more parameters fitted to experimentally observed quantities. Perdew-Burke-Ernzerhof (PBE) [14] and Becke exchange/Lee-Yang-Parr correlation (BLYP) [15] are the most popular semiempirical functionals. These functionals are successfully applied to many systems from metals to 2D self-assemblies [16]. However, it is shown that they fail to reproduce some of the experimentally observed properties of oxides accurately, due to the incorrect description of electronic localization by standard DFT [17]. The problem is the incomplete cancellation of the Coulomb self-interaction in GGA functionals, which leads to stabilization of electron delocalization [18]. For instance, PBE density functional is shown to be quite good to capture structural properties of both bulk phase and the surface of TiO$_2$; however, band gap of bulk TiO$_2$ is predicted as 1.74 eV [19] which significantly underestimates the experimentally measured band gap of 3.2 eV [20]. Therefore, for electronic structure analysis and band alignment of oxides one should go beyond GGA [21].

One of the commonly applied methods to overcome the failure of GGA is to use hybrid density functionals that mix exact exchange from Hartree-Fock exchange [22] and correlation from GGA. Applying hybrid functionals removes some of the self-interaction error and favors localized electronic states by reducing the barrier to the localization [23]. Including orbital analogue of exchange formalism in hybrid functionals often improves the accuracy of the simulations; however, computational cost increases by at least an order of magnitude with respect to the pure GGA formalism. The most popular hybrid functionals are, e.g., HSE06 [24] and PBE0 [25]. The band gap of the bulk TiO$_2$ is calculated to be 4.21 eV [26] and 3.35 eV [21]

by PBE0 and HSE06, respectively. Although larger band gaps are obtained for semiconductors using hybrid functionals, one should carefully choose the exchange-correlation formalism since significantly larger band gaps can also be obtained, e.g., PBE0.

For most of the photocatalytic applications of TiO_2, a photosensitizer or an active catalyst is adsorbed on the surface in which case both chemical and physical interactions play a role on the adsorption geometry or stability of the complex. For instance, it is shown that cis/trans coordination of the ligand with respect to anchoring group adsorbed on anatase TiO_2 (110) surface affects binding mode of the dye which likely arises due to the dispersion interactions [27]. It is well known that the exchange-correlational functionals suffer for a poor description of dispersion interactions or van der Waals interactions. To increase the accuracy of the simulations the missing dispersion interactions can also be incorporated into DFT. One way is to add dispersion energy correction term, Grimme-D3 [28], which calculates pairwise interactions between atomic species and shows usual $1/r^6$ asymptotic behavior, on top of the total energy obtained by DFT.

Using DFT, one can optimize structures, determine the most stable adsorption geometries, calculate corresponding adsorption and interaction energies, and extract electronic properties. Electronic structure can be analyzed by calculating projected density of states, which also provides energy band gaps, schematic representation of molecular orbitals, charge distribution maps, and charge density difference maps. On the other hand, the exploration of the conformational space at finite temperature is obtained by running ab-initio molecular dynamics simulations (AIMD) [29] through the generation of trajectories of several picoseconds. Phase-space trajectories are generated via numerical integration of equations of motion. Due to the advances in the electronic structure calculations, forces can be derived directly from the electrons without any empirical parameters. Within the Born-Oppenheimer approximation [30], electrons are fully decoupled from the nuclear motion at each MD step. Nuclei is subsequently propagated according to the forces obtained from the electronic structure calculation from timestep to timestep.

Although there are significant contributions to the modeling of materials/devices using many simulation methods, such as time-dependent density functional theory (TD-DFT) [31] or quantum mechanics-molecular mechanics (QM/MM) [32], it is beyond the scope of this chapter to give a complete overview of all studies with different simulation techniques. Therefore, the following sections will focus on theoretical simulations of DSSC and water splitting using DFT, sometime in combination with AIMD.

3. Theoretical simulations for photocatalytic applications of TiO_2

The photoinitiated reactions can be performed using TiO_2 as a substrate-like film having 2–3 μm thickness with 4–10 μm surface area [33], supported on another material, or in the form of nanoparticles ranging from 10 to 300 nm [34] depending on the preparation conditions [35]. There are three main stable crystal phases of TiO_2 rutile, anatase, and brookite, that being interested in heterogeneous catalytic processes. We consider the interactions at the TiO_2 surfaces, and that the most stable surfaces, i.e., the exposed surfaces of TiO_2 films or nanoparticles are the rutile (110) and anatase (101) surfaces [36]. Among these surfaces, the most stable one is known

to be the rutile and this is also the reason why it is easier to grow high quality single crystal thin films of rutile exposing the (110) surface [37]. Regarding the electronic structures, the band gaps of rutile and anatase are very similar, ≈3.2 eV; in the case of nanoparticles, some effects due to the finite size might appear, for example, the band gap increases slightly and becomes 3.35 eV [38].

For photocatalytic applications of TiO$_2$, the anatase phase is often preferred to the rutile phase because of its higher activity [39]. This characteristic is attributed to the its larger conduction band (CB) edge energy [40]. On the other hand, the comparison of DSSC performance of rutile and anatase films shows that their voltage and current characteristics are very similar. The overall solar energy conversion efficiency of rutile is only a few percentage lower than the efficiency of the anatase cell [41]. Given the relatively small difference in activity, rutile and anatase phases are the most widely explored phases of TiO$_2$. Therefore, in the following sections, we are going to consider only the anatase and rutile TiO$_2$ polymorphs.

3.1. Dye sensitized solar cells

3.1.1. Historical overview

DSSCs are obviously an important and promising application area of TiO$_2$, converting photon energy to electric energy. The very first examples of DSSCs have been developed in 1954 by Rappaport and coworkers [42]. Gallium arsenide (GaAs)-based p-n junctions, which are formed by joining n-type and p-type semiconductors, were proposed providing a solar energy conversion efficiency of 6%. The main drawback of such a system has always been its high fabrication cost on a large scale, thus preventing its commercialization. In 1991, O'Regan and Grätzel [43] proposed the today's known modern photovoltaic cell based on a n-type highly porous layer of TiO$_2$ film coated with a monolayer of dye molecules. This system can be produced at a much lower cost and it mimics photosynthesis providing a photon energy conversion efficiency of 7% under sunlight and 12% under diffuse natural light. Dye molecules absorb photons in the visible light region, while TiO$_2$ nanoparticles are employed to harvest the excited electrons from the dye's conduction band. The large band gap of TiO$_2$ is overcome by anchoring the dye to the TiO$_2$ exposed surfaces by means of properly chosen linking groups, dyes to the device are chemically stabilized on oxide nanoparticles by anchoring groups, for instance by carboxylates. Another advantage with respect to the GaAs-based photovoltaic cells is the extremely thin layer of dye molecules on a TiO$_2$ substrate which facilitates photosensitization and the electron injection into the TiO$_2$ conduction band with an efficiency of close to unity [44]. The early discovery of these interesting features and of the advances obtained by the efficient combined dye/TiO$_2$ systems, the research in this area has been strongly supported and it has led to significant progress in the field of photovoltaics.

3.1.2. Working principle of DSSC

A schematic representation of the most common TiO$_2$-based DSSC is shown in **Figure 1(a)** where the working principle of DSSC is also illustrated. A transparent conductive oxide (TOC) layer, commonly treated with a glass sheet, is the anode that is exposed to photons in the visible spectrum [45]. A mesoporous layer of TiO$_2$ nanoparticles is deposited over the TCO layer. In order to facilitate the photosensitization, dye molecules having relatively small band gap are
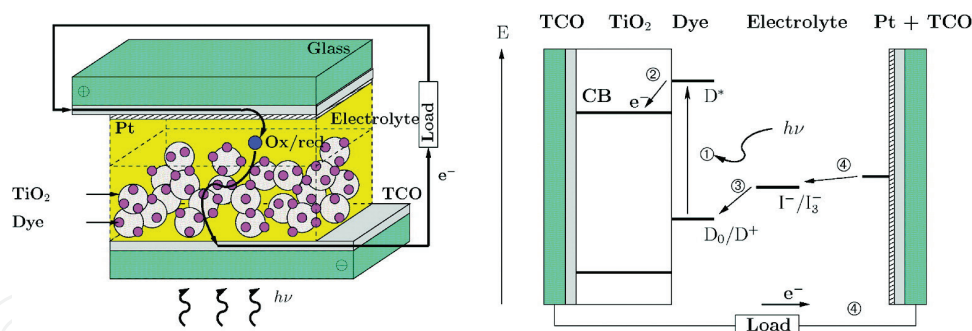
Figure 1. DSSC schematic (left) structure and (right) working principles. TCO stands for transparent conducting oxide. Reprinted with the permission from Ref. [46]. Copyright (2012) American Chemical Society.

chemically bonded to the surface of TiO$_2$ nanoparticles. The environment is filled with an electrolyte solution, typically consisting of acetonitrile as a solvent and iodine/triiodide (I$^-$/I$_3^-$) as a redox couple. The electrolyte is responsible for the regeneration of the dye molecules. The cathode part consists of TOC and an effective catalyst, generally Pt, to collect electrons from the anode.

Exposure to sunlight leads to charge separation in the dye molecules, thus generating excited electrons (e^-) in the conduction band (CB) and electron vacancies, holes (h$^+$) in the valence band (VB) of the dye. The photogenerated electrons are injected into the TiO$_2$ CB, thanks to the characteristic ultrafast electron transfer (fs timescale) [47]. Through the oxide, the electrons can be transferred to the TOC at the anode part [48]. This is known as the indirect mechanism. The direct electron injection from the VB of dye into the CB of TiO$_2$ is also possible which is reported to be faster than an indirect mechanism [49]. Transferring electrons from the anode to the cathode creates an electric current. The photogenerated holes in dye molecules combine with the electrons in 3I$^-$, oxidizing 3I$^-$ to I$_3^-$. The electrons at the Pt cathode reduce I$_3^-$ to 3I$^-$ so that regeneration of the electrolyte solution is also completed. Thanks to this working principle, solar energy is converted to an electric current in a complete cycle.

In order to be efficient, the described devise has to satisfy some essential conditions. The absorption spectra of the photosensitizers should have a good overlap with the whole solar light spectrum and some of the near-infrared regions. Moreover, the dyes should have high molar extinction coefficient, which is a measure of how strongly a substance absorbs light at a given wavelength per molar concentration. The dye's chemical stability is an another important feature, which affects the lifetime of the device. This can be achieved by chemically linking dyes and semiconductors using anchoring groups. In addition to the chemical stability, properly chosen anchoring groups might also strengthen the degree of coupling between the dyes and oxides thus enhancing the electron injection into the semiconductor CB [50].

It is necessary for a photosensitizer to promote electron injection into TiO$_2$ layers efficiently. The dye's LUMO has to be aligned correctly if the anchoring group is present, then also its LUMO alignment matters, in particular it has to be energetically close to the dye's LUMO and probably partially overlapping. Besides, the LUMO of the dye should be higher than the CB edge of the oxide to make the electron injection possible. To achieve proper regeneration of the dye, its highest occupied molecular orbital (HOMO) should be below HOMO of the redox mediator, see **Figure 1(b)** for illustration of the complete charge transfer mechanism.

3.1.3. Insights on DSSC components

Dye molecules are relatively well understood with respect to the complex surface structures of TiO$_2$ phases. The commonly used photosensitizers are either metal-free organic donor-acceptor dyes, such as polythiophenes [51], polypyrroles [52], azobenzene, catechol, and anthraquinone [53] or transition-metal based ligand complexes, such as Ru-polypyridyl molecules [54]. The metal-free organic dyes have large π conjugation leading to π-π^* transitions following the photon absorption. Higher extinction coefficients can be obtained by functionalizing metal-free organic dyes using different donor-acceptor groups, introducing heteroaromatic groups, or changing the number of double bonds in the dye structure thus enabling absorption spectra tuning [33]. Recent advances in designing purely organic dyes adsorbed on nanocrystalline TiO$_2$ result in achieving solar to power conversion efficiency of 9.5% using indoline dye by Ito et al. [55] and 9.8% using thienothiophene conjugated chromophore by Zhang et al. [56]

Transition metal-based dyes show higher efficiencies with respect to their fully organic counterparts. This is attributed to their capability of absorption in large spectrum range from the visible to the near-infrared regime. The ligand system, i.e., polypyridyl-based or phthalocyanine-based, can be complexed with a chosen transition metal, i.e., Ru, Zn, Mg, and Co. The possibility of long-lived metal-to-ligand (MLCT), d-π^*, or ligand-to-ligand (LLCT), π-π^*, charge transfer once exposed to solar light makes them promising candidates for DSSC applications. However, all these advantages come with a cost, such as the presence of expensive transition metal, i.e., Ru, and rather difficult synthesis and purification steps. Nontoxic and cheap natural dyes that are already present in vegetables and fruits are another possibility to consider. However, unlike synthetic dyes, their recorded efficiency is only around 2% [57].

As already stated, dye molecules are bound to the TiO$_2$ surface by anchoring groups to enhance chemical stability of the complex. The anchoring groups should be well chosen, since the presence of water in electrolyte solution may weaken the binding strength of the anchors to the TiO$_2$ surface thus leading to desorption of the dye molecules. Phosphonate groups have been proposed for anchoring Ru-dye/TiO$_2$ complex and shown to be better candidates than carboxylates [58]. Formic acids are another common example of anchoring groups used in DSSCs [59]. In addition to chemical stability, anchoring groups also affect the degree of coupling between the dye and the semiconductor, which promotes/hinders electron injection into oxide CB. It is shown that strong coupling between Ru-based dyes and TiO$_2$ nanoparticles anchored by carboxylates leads to an electron injection on femtosecond timescale. On the other hand, SnO$_2$ and ZnO thin films having lower density of states coupled to a dye/anchoring group have much slower electron injection time with respect to TiO$_2$ [60].

3.1.4. Simulation studies for DSSC

Up to date, Ru-based dyes such as N3 and N749 are the most widely investigated dyes with recorded efficiency of 11.4% [61]. Labat et al. [62] studied the electronic and structural properties of N3 dye on anatase (101) surface using DFT. As depicted in **Figure 2** while computed orbitals of the HOMO and HOMO-1 are centered on N3 dye and correspond to a t_{2g}-π^* interaction between Ru and the ligand, the LUMO is distributed over anatase slab. This picture
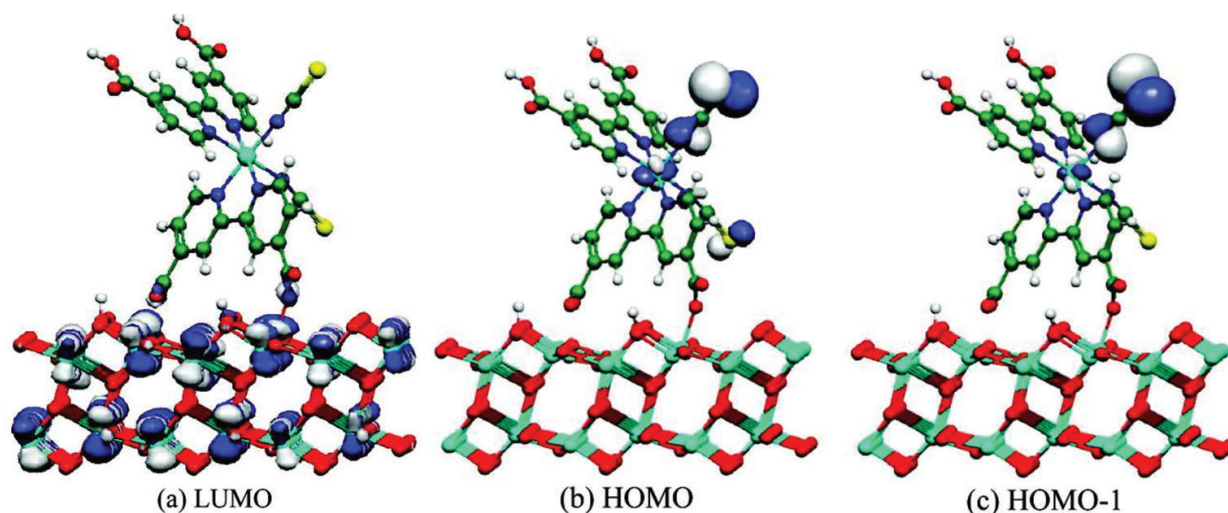
Figure 2. Calculated (a) LUMO, (b) HOMO, and (c) HOMO-1 crystalline orbitals for the bridging adsorption mode of N3/TiO$_2$\rm_2. Isovalues: |0.040| and |0.007| for HOMOs and LUMOs, respectively. Reprinted with the permission from Ref. [62]. Copyright (2010) American Chemical Society.

suggests a favorable electron transfer from the HOMO of the dye to the LUMO of the TiO$_2$. Schiffmann et al. [27] modeled N3, N712, and N719 dyes adsorbed on anatase (101) surface in the presence of solvent acetonitrile using AIMD. Results indicate that the dyes that are doubly bound to the pristine anatase surface have higher stability. On the other hand, addition of surface protons changes adsorption geometry and mixed bidentate and monodentate binding modes become more favorable. Similarly, the modeling of protonated/deprotonated different N749/(TiO$_2$)$_{28}$ structures shows that the complexes with deprotonated dye molecules are more favorable with higher adsorption energies [63]. Lundqvist et al. [50] investigated the effects of several spacer unit and anchoring group combinations on the interfacial electronic coupling between a set of Ru^{II}-(tpy)$_2$ dyes and (TiO$_2$)$_{46}$ nanocrystal. Calculations show that while the strongest coupling is observed using a carboxylic acid anchoring group without a spacer unit, the weakest coupling is observed with the combination of the phosphonic acid anchor group and phenylene spacer group. A good comparison of the calculated structural and electronic characteristics of several Ru-based dyes and their interactions with TiO$_2$ is available in a recent review [64].

Although Ru-based photosensitizers are very often explored in the literature because of their specific photophysical characteristics and their better performance [65, 66], there are other studies which try to replace expensive Ru metal with cheaper transition metals, such as Fe, Cu, and Co. The experimental study of Ferrere and Gregg [67] investigating Fe(II)bipyridine molecule adsorbed onto nanocrystalline TiO$_2$ films reveals the substandard performance of Fe-based dyes. The low performance of Fe-based dyes is attributed to the weaker ligand field which prevents MLCT state populations. While the strong ligand field in Ru-based dyes results in having nanoseconds to microseconds lifetime of excited states, excited state lifetime in Fe(II)bipyridine is shown to be only around ps timescale. In spite of the lower performance of the cheaper transition-metal deposited dyes, there are several theoretical studies investigating structural and electronic properties of the most promising ones.

Guillemoles et al. [68] modeled the Os-based polypyridyl dyes with different linker groups (CN⁻ vs. NCS⁻) and in different environments (gas vs. aqueous solution). Their study shows the effects of linker groups and environment on the structural and electronic properties of the dyes. Although in the gas phase the Os-CN⁻ distance becomes shorter than Os-NCS⁻ due to the better electron donation character of CN⁻, aqueous solution leads to contraction of Os-CN⁻ (Os-NCS⁻) bonds and increases the Os-pyridine distances. Calculated HOMO has contribution from both Os and the linkers, while the LUMO is located on the bipyridyl ligand with π^* character. Shalabi et al. [69] compared the optimized structures of Zn-based porphyrin (ZnPor) and porphyrazin (ZnPz) macrocycles and their energy gaps using DFT. They showed that band gap becomes narrower for ZnPz with respect to ZnPor by more than 0.8 eV, which suggests that light harvesting efficiency can be increased by replacing porphyrin ligand with porphyrazin. Lu et al. [70] compared the electronic structures of several polypyridyl-based dyes with Cu and Ru metal centers. HOMO-LUMO gaps of all considered Cu-based dyes are within the range of 2.41–2.93 eV providing properly aligned energies of the HOMO and LUMO with respect to the electrolyte solution and the CB of TiO₂, respectively. The optical characteristics of Cu and Ru-based dyes are shown to be similar in this study thus providing motivation for the future works on abundant metal-centered dyes.

Fully organic dyes are the alternative of the transition metal deposited ones. One of the widely studied metal-free dyes is catechol. The band gap of catechol, ≈4.2 eV, is larger than the TiO₂ band gap; however, it is shown that the absorption spectra of the catechol/TiO₂ complex have an intense band at 2.95 eV [71]. This observation is explained by a direct electron injection into the CB of TiO₂ from the catechol VB [72]. A DFT study by Persson et al. [73] attributes the reason of direct electron injection to the occupied π level of the catechol at the lower end of the anatase band gap. In terms of adsorption geometry, it is shown that two possible stable catechol monolayer structures present on the rutile TiO₂ (110) surface are monodentate only or mixed monodentate-bidentate configurations [74].

Oprea et al. [75] investigated several coumarin-based dyes adsorbed on different sizes of anatase (101) nanoparticles. Preferential adsorption mode of the coumarin dyes is determined as bidentate bridging which results in localization of the HOMO state on the dyes and the LUMO on the substrate. De Angelis et al. [76] modeled squaraine dye adsorbed on anatase (101) slab in water environment using AIMD. They showed that adsorption mode of squaraine changes from bridged bidentate to a monodentate as simulation time evolves. After 6 ps, however, squaraine is desorbed from the surface due to the strong solvent reorganization which weakens the binding strength of the anchoring group, carboxylic acid.

3.2. Photocatalytic water splitting

Molecular hydrogen has the highest specific energy content as compared to other energy carriers such as electricity and biofuels, conventional fuels such as coal and oil or renewable energy sources as, for example, wind and biomass. Dihydrogen is also environmentally friendly because, the waste product after its reaction with pure dioxygen is only water. These features make H₂ a potential candidate for energy carrier in the near future. One of the dihydrogen generation methods is photochemical water splitting [77]. Several transition metal

deposited catalysts such as porphyrin-derived molecules [78], cobaloximes [79], pyrphyrins [80], and molecules with polypyridine ligands [81] have been used for hydrogen evolution in homogeneous environment. Alternatively, to prevent photogenerated charge recombination and stabilize the system and reaction intermediate heterogeneous systems have been widely investigated.

Water splitting on the bare TiO_2 surface is thermodynamically allowed; however, due to the large overpotential for both H_2 and O_2, the reaction is kinetically hindered. Therefore, the pristine TiO_2 surface is inactive for water splitting and needs to be functionalized with metals/nonmetals, large macrocyclic molecules, or mixed with other types of oxides. Several studies deduce the design criteria for an efficient overall water splitting devise based on TiO_2 which can be summarized, as its valence band maximum should be more positive than the oxidation potential of water and its conduction band minimum should be more negative than the reduction potential of a proton [82].

In 1972, Fujishima and Honda [83] carried out the successful and inspiring experiment of water splitting using TiO_2 as a photoanode. In a closed circuit photoelectrochemical cell, photogenerated electron and hole pairs move to the TiO_2 surface where water molecules are oxidized to generate O_2 and resultant protons are combined with electrons at the cathode, Pt, to generate H_2. The correlation has been observed between the band gaps of the photoanode and its water splitting activity. If the band gap becomes closer to the free energy of the water splitting reaction, 1.23 eV, then the efficiency of the photoelectrochemical cell becomes relatively high, around 41%. Efficiency drops to 18% for a band gap of 2 eV. Further increase in the band gap, 3 eV, results in dramatic decrease in the efficiency of the cell, 0.05% [84]. These results engender band gap tuning of TiO_2 by taking advantage of several methods, as discussed below.

An alternative to the photoelectrochemical cells proposed by Fujishima and Honda [83], two other widely explored methods of water splitting using TiO_2 have been recommended. One method is to use transition metal-deposited TiO_2 nanoparticles together with another metal oxide. An example is depicted in **Figure 3(a)** where photon absorption is followed by charge
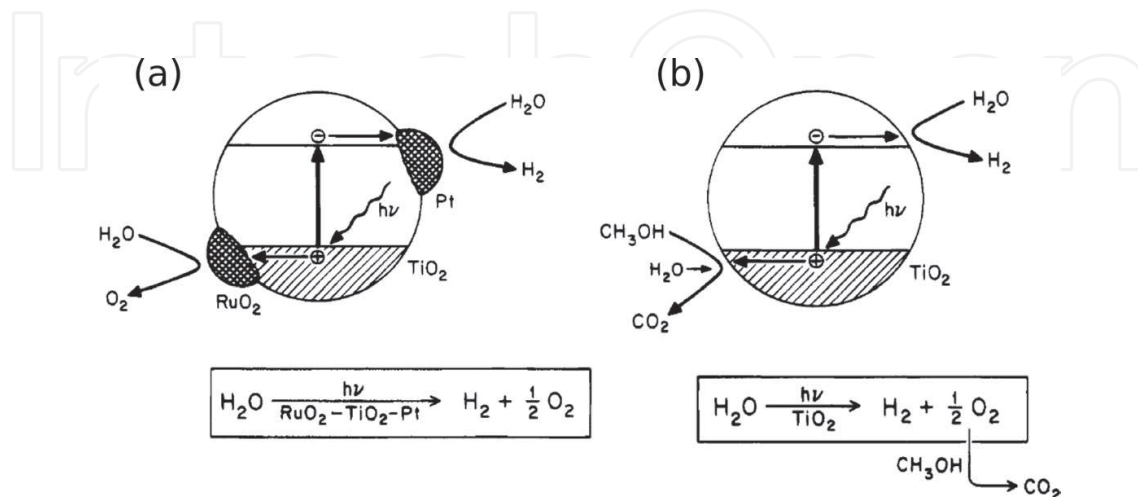
Figure 3. (a) Photosplitting of water on a composite catalyst. (b) Photosplitting of water: sacrificial donor effect. Reprinted with the permission from Ref. [85]. Copyright (1995) American Chemical Society.

separation in TiO$_2$ and photogenerated electrons and holes are transported into Pt for H$_2$ generation and RuO$_2$ for O$_2$ evolution, respectively. This design results in a substantial decrease in overpotential of the reaction [85]. Another proposed method is to use sacrificial agents to remove one of the photogenerated products. An illustration is shown in **Figure 3(b)** where CH$_3$OH is used as a sacrificial specie. While photogenerated holes are injected into CH$_3$OH which afterwards oxidizes water, excited electrons in TiO$_2$ CB reduces water to H$_2$ [85]. This system focuses on half reactions, either water reduction via sacrificial electron donor or water oxidation via sacrificial electron acceptor [86].

Prior to reviewing theoretical studies of water splitting on functionalized TiO$_2$ surfaces, it is useful to first give a closer examination of the interactions between water molecules and the pristine TiO$_2$ surface. It is shown that water molecules prefer to adsorb on oxygen vacancies of the rutile (110) surface [87]. Water adsorption is followed by a proton transfer to the adjacent two-coordinated surface oxygen thus leading to a formation of hydroxy radical on the surface [88]. Zhao [89] calculated adsorption and decomposition energies of water molecules on different rutile surfaces, such as (110), (100), and (001) using DFT. While dissociative adsorption of water is more favorable on the (110) surface, the activation energy of the water dissociation is largest on the (100) surface. Calculations by Hahn et al. [90] showed that the employed adsorbate coverage affects the favored adsorption mechanism of water molecules. While at low coverage water molecules tend to dissociate on the rutile (110) surface, increasing coverage leads to an associative adsorption. Investigating interactions between water and bare TiO$_2$ surface is a fundamental research; however, for photocatalytic water splitting TiO$_2$ surface has to be functionalized, as stated earlier.

Adsorption of large macrocyclic water reduction/oxidation catalysts on the TiO$_2$ surface is shown to be a promising way of achieving the water splitting reaction. In this regard, Monti et al. [91] proposed a model system of Ru-based catalyst/antenna/TiO$_2$ complex for water splitting and investigated proton coupled electron transfer dynamics of the catalyst in water solution using AIMD. Results show that a water molecule binds to the Ru center and after 1.9 ps of simulation, time proton transfer from the attached water molecule to the closest one in the solution is achieved. Gurdal et al. [21] modeled adsorption of co-deposited pyrphyrin (CoPyr), a water reduction catalyst [80], on the rutile TiO$_2$ (110) surface using DFT. The band gap of the complex is decreased by more than 1.5 eV with respect to the bare surface. Additionally, the catalytic properties of CoPyr are preserved upon adsorption since the adsorption process does not lead to strong modifications of the electronic structure at the Co(II) active center.

Alternative complexes, metal/nonmetal deposited TiO$_2$ structures, are investigated by many groups. Phase stabilities of Fe, Al, Si, and F deposited rutile and anatase phases of TiO$_2$ are compared using DFT [92]. Results show that while cationic dopants in Ti lattice sites stabilize anatase slightly more than rutile, anionic doping with F substantially reduces the phase stability of the anatase. Modeling Pt, Ru, and Co ions doped anatase TiO$_2$ (001) surface shows that band gaps of the complexes decrease in the order of deposition of Co (by 1.8 eV), Ru (by 1.7 eV), and Pt (by 0.4 eV) [93]. Nucleation and growth mechanism of Ru clusters on the anatase TiO$_2$(101) surface reveals that in addition to decrease in the band gap, an electron accumulation at the metal/oxide interface is observed due to the electron flow from Ru to TiO$_2$ [94].

There are also other studies that focus on designing water splitting systems by mixing TiO_2 with another metal oxide. Graciani et al. [95] modeled water adsorption on the Ce_2O_3 doped rutile $TiO_2(110)$ surface. Results show that the proposed mixed-metal oxide has a promising ability to dissociate water exposing an exothermic dissociation energy of −0.7 eV with a small activation barrier of 0.04 eV. A relatively larger system is investigated by Pastore and De Angelis [96] who modeled TiO_2/Ru-dye/IrO_2 complex using DFT. In the designed complex Ru polypyridyl dye, acting as a linker between the oxides, is attached to both the anatase $TiO_2(101)$ and IrO_2 surfaces via phosphonic acid and malonate groups, respectively. **Figure 4** shows the orientation of the Ru-dye with respect to the oxides. Electronic structure analysis shows that both the HOMO and LUMO are located on IrO_2 showing a metallic-like character. While the occupied molecular orbitals of the dye are located within the IrO_2 VB, its unoccupied orbitals are distributed over the CB of both IrO_2 and TiO_2.
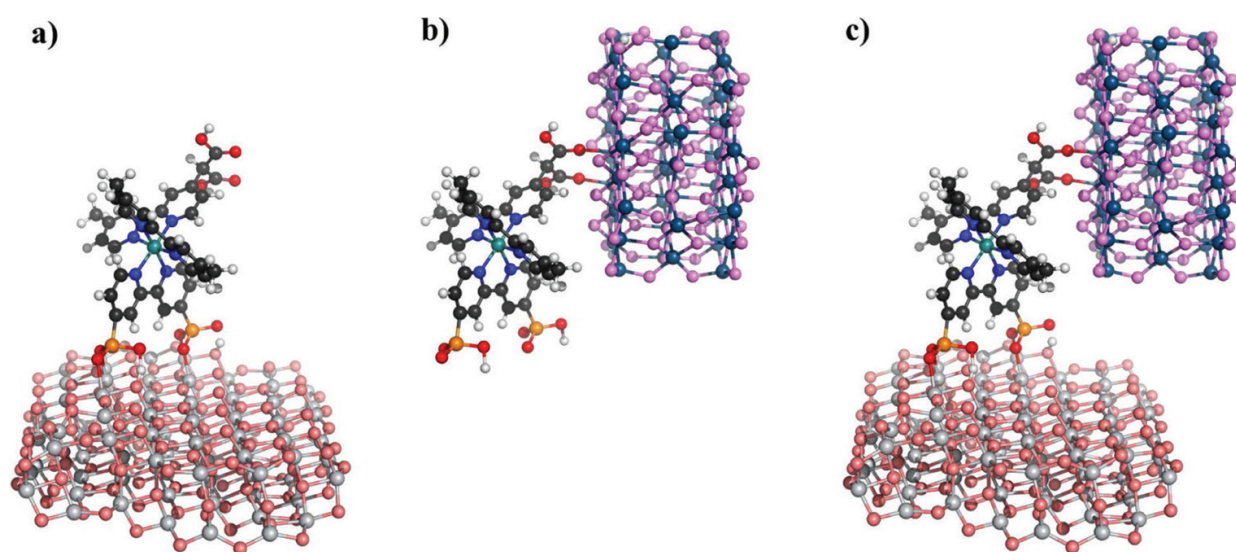
Figure 4. Optimized molecular structure of Ru-dye in its partially deprotonated form, grafted to the $(TiO_2)_2 {82}_2$ cluster (a), to the $(IrO2_2)_2 {56}_2.2H_2O$ nanoparticle (b), and tethered across the TiO_2 and IrO_2 systems, (c). Reprinted with the permission from Ref.~\cite{pastore2015} Copyright (2015) American Chemical Society

4. Challenges of DFT-based simulations

In order to understand the physical properties of TiO_2 complexes and develop photocatalytically active and efficient devices, one has to use adequate theoretical methods. Although DFT is a powerful tool to analyze and screen TiO_2-based complexes for photocatalytic applications, it also has some limitations. Accurate results can be obtained by increasing system size, i.e., increasing layers of the TiO_2 slab. While the thickness of the slab has to be sufficient to reproduce the correct behavior at the surface and increase the calculated accuracy, increasing system size also increases computational effort. In the case of AIMD runs required computational source becomes even more expensive than DFT calculations. Therefore, one needs to find a compromise between the accuracy and the computational cost. In this regard, Harris

and Quong [97] proposed a method named "25% rule" to determine the sufficient slab thickness that should be used in the simulations.

As already stated, the other issue is the uncertain forms of the exchange-correlation functionals which limit the accuracy and cause a dilemma in trusting obtained results. Though, several methods beyond DFT are developed and successfully used to increase the accuracy of the calculations, such as random phase approximation and Green function theory [98, 99].

In spite of several limitations, in both the accuracy of the DFT description and the size of feasible models, this approach seems to be the most appropriate one so far. Constant improvement in computational algorithms together with rapidly increasing computer power, DFT, and AIMD are robust methods used to gain preliminary knowledge on the systems and supervise experimentalists to build promising materials for photocatalytic applications.

5. Conclusions

Search for renewable energy sources leads scientists to benefit from sunlight and convert photon energy to chemical/electric energy using TiO$_2$-based materials. Although photocatalytic water splitting and DSSC applications are accomplished using TiO$_2$ surface, large band gap of the oxide limits absorbing photons in the visible spectrum thus hindering device efficiency. Therefore, functionalizing TiO$_2$ surface by adsorbing photosensitizers and/or water reduction/oxidation catalysts, by metal/nonmetal deposition, or by mixing with other oxides, the optical response of the complex can be shifted from UV to the visible region. This is the crucial requirement in designing promising, robust, and scalable photocatalysts toward water splitting and DSSC applications.

Together with the improvement in the computational power, today, DFT is an important tool to obtain optimized geometries of the complexes, analyze electronic structures, model many spectroscopic techniques, determine intermediate states of the reactions, and so on. In particular, it is powerful for modeling several TiO$_2$-based materials and testing their physical/chemical/optical characteristics for photocatalytic applications. Although there are some limitations in DFT, several new exchange-correlation density functionals and van der Waals correction schemes have been proposed to increase the flexibility and accuracy of the model. Using DFT, all phases of TiO$_2$ surfaces, i.e., rutile, anatase, and TiO$_2$ nanoparticles can be modeled. The outcome of the simulations serves as an initial knowledge on the systems for scientists without experimental effort.

Author details

Yeliz Gurdal* and Marcella Iannuzzi

*Address all correspondence to: yeliz.guerdal@chem.uzh.ch

Department of Chemistry, University of Zurich, Zürich, Switzerland

References

[1]　Goodeve CF, Kitchener JA. The mechanism of photosensitisation by solids. Transactions of the Faraday Society. 1938;**34**:902-908. DOI: 10.1039/TF9383400902

[2]　Fujiyoshi S, Ishibashi TA, Onishi H. Fourth-order Raman spectroscopy of wide-band gap materials. The Journal of Physical Chemistry B. 2005;**109**:8557-8561. DOI: 10.1021/jp051203i

[3]　Iman-Amir M, Julkapli N, Bagheri S, Yousefi AT. TiO_2 hybrid photocatalytic systems: Impact of adsorption and photocatalytic performance. Reviews in Inorganic Chemistry. 2015;**35**:151-178. DOI: 10.1515/revic-2015-0005

[4]　Li LL, Diau EWG. Porphyrin-sensitized solar cells. Chemical Society Reviews. 2013;**42**:291-304. DOI: 10.1039/C2CS35257E

[5]　Imahori H, Kang S, Hayashi H, Haruta M, Kurata H, Isoda S, et al. Photoinduced charge carrier dynamics of Zn-Porphyrin-TiO_2 electrodes: The key role of charge recombination for solar cell performance. The Journal of Physical Chemistry A. 2011;**115**:3679-3690. DOI: 10.1021/jp103747t

[6]　Hohenberg P, Kohn W. Inhomogeneous electron gas. Physical Review. 1964;**136**:B864-B871. DOI: 10.1103/PhysRev.136.B864

[7]　Kohn W, Sham LJ. Self-consistent equations including exchange and correlation effects. Physical Review. 1965;**140**:A1133-A1138. DOI: 10.1103/PhysRev.140.A1133

[8]　Giannozzi P, Baroni S, Bonini N, Calandra M, Car R, Cavazzoni C, et al. QUANTUM ESPRESSO: A modular and open-source software project for quantum simulations of materials. Journal of Physics: Condensed Matter. 2009;**21**:395502-395520

[9]　Lippert G, Hutter J, Parrinello M. A hybrid Gaussian and plane wave density functional scheme. Molecular Physics. 1997;**92**:477-488. DOI: 10.1080/002689797170220

[10]　Iannuzzi M, Hutter J. Comparative study of the nature of chemical bonding of corrugated graphene on Ru(0001) and Rh(111) by electronic structure calculations. Surface Science. 2011;**605**:1360-1368. DOI: 10.1016/j.susc.2011.04.031

[11]　Mette G, Sutter D, Gurdal Y, Schnidrig S, Probst B, Iannuzzi M, et al. From porphyrins to pyrphyrins: Adsorption study and metalation of a molecular catalyst on Au(111). Nanoscale. 2016;**8**:7958-7968. DOI: 10.1039/C5NR08953K

[12]　Becke AD. A new mixing of Hartree-Fock and local density-functional theories. The Journal of Chemical Physics. 1993;**98**:1372-1377. DOI: 10.1063/1.464304

[13]　Perdew JP, Yue W. Accurate and simple density functional for the electronic exchange energy: Generalized gradient approximation. Physical Review B. 1986;**33**:8800-8802. DOI: 10.1103/PhysRevB.33.8800

[14]　Perdew JP, Burke K, Ernzerhof M. Generalized gradient approximation made simple. Physical Review Letters. 1996;**77**:3865-3868. DOI: 10.1103/PhysRevLett.77.3865

[15] Lee C, Yang W, Parr RG. Development of the Colle-Salvetti correlation-energy formula into a functional of the electron density. Physical Review B. 1988;**37**:785-789. DOI: 10.1103/PhysRevB.37.785

[16] Iannuzzi M, Tran F, Widmer R, Dienel T, Radican K, Ding Y, et al. Site-selective adsorption of phthalocyanine on h-BN/Rh(111) nanomesh. Physical Chemistry Chemical Physics. 2014;**16**:12374-12384. DOI: 10.1039/C4CP01466A

[17] Skorodumova NV, Ahuja R, Simak SI, Abrikosov IA, Johansson B, Lundqvist BI. Electronic, bonding, and optical properties of CeO$_2$ and Ce$_2$O$_3$ from first principles. Physical Review B. 2001;**64**:115108-115116. DOI: 10.1103/PhysRevB.64.115108

[18] Ganduglia-Pirovano MV, Da Silva JLF, Sauer J. Density-functional calculations of the structure of near-surface oxygen vacancies and electron localization on CeO$_2$(111). Physical Review Letters. 2009;**102**:26101-26104. DOI: 10.1103/PhysRevLett.102.026101

[19] Evarestov RA, Zhukovskii YF. Four-faceted nanowires generated from densely-packed TiO$_2$ rutile surfaces: Ab initio calculations. Surface Science. 2013;**608**:226-240. DOI: 10.1016/j.susc.2012.10.012

[20] Kavan L, Grätzel M, Gilbert SE, Klemenz C, Scheel HJ. Electrochemical and photoelectrochemical investigation of single-crystal anatase. Journal of the American Chemical Society. 1996;**118**:6716-6723. DOI: 10.1021/ja954172l

[21] Gurdal Y, Luber S, Hutter J, Iannuzzi M. Non-innocent adsorption of co-pyrphyrin on rutile(110). Physical Chemistry Chemical Physics. 2015;**17**:22846-22854. DOI: 10.1039/C5CP02767E

[22] Slater JC. A Simplification of the Hartree-Fock method. Physical Review. 1951;**81**:385-390. DOI: 10.1103/PhysRev.81.385

[23] Da Silva JLF, Ganduglia-Pirovano MV, Sauer J, Bayer V, Kresse G. Hybrid functionals applied to rare-earth oxides: The example of ceria. Physical Review B. 2007;**75**:45121-45130. DOI: 10.1103/PhysRevB.75.045121

[24] Heyd J, Scuseria GE, Ernzerhof M. Hybrid functionals based on a screened Coulomb potential. The Journal of Chemical Physics. 2003;**118**:8207-8215. DOI: 10.1063/1.1564060

[25] Ernzerhof M, Scuseria GE. Assessment of the Perdew–Burke–Ernzerhof exchange-correlation functional. The Journal of Chemical Physics. 1999;**110**:5029-5036. DOI: 10.1063/1.478401

[26] Bahers TL, Rérat M, Sautet P. Semiconductors used in photovoltaic and photocatalytic devices: Assessing fundamental properties from DFT. The Journal of Physical Chemistry C. 2014;**118**:5997-6008. DOI: 10.1021/jp409724c

[27] Schiffmann F, VandeVondele J, Hutter J, Wirz R, Urakawa A, Baiker A. Protonation-dependent binding of ruthenium bipyridyl complexes to the anatase(101) surface. The Journal of Physical Chemistry C. 2010;**114**:8398-8404. DOI: 10.1021/jp100268r

[28] Grimme S, Antony J, Ehrlich S, Krieg H. A consistent and accurate ab initio parametrization of density functional dispersion correction (DFT-D) for the 94 elements H-Pu. The Journal of Chemical Physics. 2010;**132**:154104-154122. DOI: 10.1063/1.3382344

[29] Kirchner B, di Dio PJ, Hutter J. Real-World predictions from ab initio molecular dynamics simulations. In: Kirchner B, Vrabec J, editors. Multiscale Molecular Methods in Applied Chemistry. Berlin, Heidelberg: Springer; 2012. pp. 109-153. DOI: 10.1007/128-2011-195

[30] Barnett RN, Landman U. Born-Oppenheimer molecular-dynamics simulations of finite systems: Structure and dynamics of $(H_2O)_2$. Physical Review B. 1993;**48**:2081-2097. DOI: 10.1103/PhysRevB.48.2081

[31] Burke K, Werschnik J, Gross EKU. Time-dependent density functional theory: Past, present, and future. The Journal of Chemical Physics. 2005;**123**:62206-62214. DOI:10.1063/1.1904586

[32] Lin H, Truhlar DG. QM/MM: What have we learned, where are we, and where do we go from here? Theoretical Chemistry Accounts. 2006;**117**:185. DOI:10.1007/s00214-006-0143-z

[33] Mishra A, Fischer Mâ, Bäuerle P. Metal-free organic dyes for dye-sensitized solar cells: From structure: Property relationships to design rules. Angewandte Chemie International Edition. 2009;**48**:2474-2499. DOI:10.1002/anie.200804709

[34] Liao DL, Liao BQ. Shape, size and photocatalytic activity control of TiO_2 nanoparticles with surfactants. Journal of Photochemistry and Photobiology A: Chemistry. 2007;**187**:363-369. DOI: 10.1016/j.jphotochem.2006.11.003

[35] Barnard AS, Curtiss LA. Prediction of TiO_2 nanoparticle phase and shape transitions controlled by surface chemistry. Nano Letters. 2005;**5**:1261-1266. DOI: 10.1021/nl050355m

[36] Esch TR, Gadaczek I, Bredow T. Surface structures and thermodynamics of low-index of rutile, brookite and anatase – A comparative DFT study. Applied Surface Science. 2014;**288**:275-287. DOI: 10.1016/j.apsusc.2013.10.021

[37] Lazzeri M, Vittadini A, Selloni A. Structure and energetics of stoichiometric TiO_2 anatase surfaces. Physical Review B. 2001;**63**:155409-155417. DOI: 10.1103/PhysRevB.63.155409

[38] Kormann C, Bahnemann DW, Hoffmann MR. Preparation and characterization of quantum-size titanium dioxide. The Journal of Physical Chemistry. 1988;**92**:5196-5201. DOI: 10.1021/j100329a027

[39] Luttrell T, Halpegamage S, Tao J, Kramer A, Sutter E, Batzill M. Why is anatase a better photocatalyst than rutile? - Model studies on epitaxial TiO_2 films. Scientific Reports. 2014;**4**:4043-4050. DOI: 10.1038/srep04043 10.1038/srep04043

[40] Wold A. Photocatalytic properties of titanium dioxide (TiO_2). Chemistry of Materials. 1993;**5**:280-283. DOI: 10.1021/cm00027a008

[41] Park NG, van de Lagemaat J, Frank AJ. Comparison of dye-sensitized rutile and anatase-based TiO_2 solar cells. Journal of Physical Chemistry B. 2000;**104**:8989-8994. DOI: 10.1021/jp994365l

[42] Jenny DA, Loferski JJ, Rappaport P. Photovoltaic effect in GaAs *p-n* junctions and solar energy conversion. Physical Review. 1956;**101**:1208-1209. DOI: 10.1103/PhysRev. 101.1208

[43] O'Regan B, Grätzel M. A low-cost, high-efficiency solar cell based on dye-sensitized colloidal TiO$_2$ films. Nature. 1991;**353**:737-740. DOI: 10.1038/353737a0

[44] Smestad G, Bignozzi C, Argazzi R. Testing of dye sensitized TiO$_2$ solar cells I: Experimental photocurrent output and conversion efficiencies. Solar Energy Materials and Solar Cells. 1994;**32**:259-272. DOI: 10.1016/0927-0248(94)90263-1

[45] Gong J, Liang J, Sumathy K. Review on dye-sensitized solar cells (DSSCs): Fundamental concepts and novel materials. Renewable and Sustainable Energy Reviews. 2012;**16**:5848-5860. DOI: 10.1016/j.rser.2012.04.044

[46] Labat F, Le Bahers T, Ciofini I, Adamo C. First-principles modeling of dye-sensitized solar cells: Challenges and perspectives. Accounts of Chemical Research. 2012;**45**:1268-1277. DOI: 10.1021/ar200327w

[47] Shklover V, Ovchinnikov YE, Braginsky LS, Zakeeruddin SM, Grätzel M. Structure of organic/inorganic interface in assembled materials comprising molecular components. Crystal structure of the sensitizer Bis[(4,4'-carboxy-2,2'-bipyridine)(thiocyanato)] ruthenium(II). Chemistry of Materials. 1998;**10**:2533-2541. DOI: 10.1021/cm980303g

[48] Duncan WR, Prezhdo OV. Theoretical studies of photoinduced electron transfer in dye-sensitized TiO$_2$. Annual Review of Physical Chemistry. 2007;**58**:143-184. DOI: 10.1146/annurev.physchem.58.052306.144054

[49] Ghosh HN, Asbury JB, Lian T. Direct observation of ultrafast electron injection from Coumarin 343 to TiO$_2$ nanoparticles by femtosecond infrared spectroscopy. The Journal of Physical Chemistry B. 1998;**102**:6482-6486. DOI: 10.1021/jp981806c

[50] Lundqvist MJ, Nilsing M, Lunell S. Spacer and anchor effects on the electronic coupling in Ruthenium-bis-terpyridine dye-sensitized TiO$_2$ nanocrystals studied by DFT. The Journal of Physical Chemistry B. 2006;**110**:20513-20525. DOI: 10.1021/jp064045j

[51] Zhu Y, Xu S, Jiang L, Pan K, Dan Y. Synthesis and characterization of polythiophene/titanium dioxide composites. Reactive and Functional Polymers. 2008;**68**:1492-1498. DOI: 10.1016/j.reactfunctpolym.2008.07.008

[52] Wang D, Wang Y, Li X, Luo Q, An J, Yue J. Sunlight photocatalytic activity of polypyrrole–TiO$_2$ nanocomposites prepared by 'in situ' method. Catalysis Communications. 2008;**9**:1162-1166. DOI:10.1016/j.catcom.2007.10.027

[53] Jacquemin D, Perpète EA, Scuseria GE, Ciofini I, Adamo C. TD-DFT performance for the visible absorption spectra of organic dyes: conventional versus long-range hybrids. Journal of Chemical Theory and Computation. 2008;**4**:123-135. DOI: 10.1021/ct700187z

[54] Balzani V, Juris A, Venturi M, Campagna S, Serroni S. Luminescent and redox-active polynuclear transition metal complexes. Chemical Reviews. 1996;**96**:759-834. DOI: 10.1021/cr941154y

[55] Ito S, Miura H, Uchida S, Takata M, Sumioka K, Liska P, et al. High-conversion-efficiency organic dye-sensitized solar cells with a novel indoline dye. Chemical Communications. 2008;5194-5196. DOI: 10.1039/B809093A

[56] Zhang G, Bala H, Cheng Y, Shi D, Lv X, Yu Q, et al. High efficiency and stable dye-sensitized solar cells with an organic chromophore featuring a binary π-conjugated spacer. Chemical Communications. 2009;2198-2200. DOI:10.1039/B822325D

[57] Calogero G, Yum JH, Sinopoli A, Marco GD, Grätzel M, Nazeeruddin MK. Anthocyanins and betalains as light-harvesting pigments for dye-sensitized solar cells. Solar Energy. 2012;**86**:1563-1575. DOI: 10.1016/j.solener.2012.02.018

[58] Zakeeruddin SM, Nazeeruddin MK, Pechy P, Rotzinger FP, Humphry-Baker R, Kalyanasundaram K, et al. Molecular engineering of photosensitizers for nanocrystalline solar cells: Synthesis and characterization of Ru dyes based on phosphonated terpyridines. Inorganic Chemistry. 1997;**36**:5937-5946. DOI: 10.1021/ic970008i

[59] Miller KL, Falconer JL, Medlin JW. Effect of water on the adsorbed structure of formic acid on TiO_2 anatase (101). Journal of Catalysis. 2011;**278**:321-328. DOI: 10.1016/j.jcat.2010.12.019

[60] Asbury JB, Hao E, Wang Y, Ghosh HN, Lian T. Ultrafast electron transfer dynamics from molecular adsorbates to semiconductor nanocrystalline thin films. The Journal of Physical Chemistry B. 2001;**105**:4545-4557. DOI: 10.1021/jp003485m

[61] Han L, Islam A, Chen H, Malapaka C, Chiranjeevi B, Zhang S, et al. High-efficiency dye-sensitized solar cell with a novel co-adsorbent. Energy and Environmental Science. 2012;**5**:6057-6060. DOI: 10.1039/C2EE03418B

[62] Labat F, Ciofini I, Hratchian HP, Frisch MJ, Raghavachari K, Adamo C. Insights into working principles of ruthenium polypyridyl dye-sensitized solar cells from first principles modeling. The Journal of Physical Chemistry C. 2011;**115**:4297-4306. DOI: 10.1021/jp108917c

[63] Liu SH, Fu H, Cheng YM, Wu KL, Ho ST, Chi Y, et al. Theoretical study of N749 dyes anchoring on the $(TiO_2)_{28}$ surface in DSSCs and their electronic absorption properties. The Journal of Physical Chemistry C. 2012;**116**:16338-16345. DOI: 10.1021/jp3006074

[64] Fantacci S, De Angelis F. A computational approach to the electronic and optical properties of Ru(II) and Ir(III) polypyridyl complexes: Applications to DSC, OLED and NLO. Coordination Chemistry Reviews. 2011;**255**:2704-2726. DOI: 10.1016/j.ccr.2011.03.008

[65] Hagfeldt A, Grätzel M. Molecular photovoltaics. Accounts of Chemical Research. 2000;**33**:269-277. DOI: 10.1021/ar980112j

[66] Karlsson S, Boixel J, Pellegrin Y, Blart E, Becker HC, Odobel F, et al. Accumulative charge separation inspired by photosynthesis. Journal of the American Chemical Society. 2010;**132**:17977-17979. DOI: 10.1021/ja104809x

[67] Ferrere S, Gregg BA. Photosensitization of TiO_2 by [FeII(2,2'-bipyridine-4,4'-dicarboxylic acid)$_2$(CN)$_2$]: Band selective electron injection from ultra-short-lived excited states. Journal of the American Chemical Society. 1998;**120**:843-844. DOI:10.1021/ja973504e

[68] Guillemoles JF, Barone V, Joubert L, Adamo C. A theoretical investigation of the ground and excited states of selected Ru and Os polypyridyl molecular dyes. The Journal of Physical Chemistry A. 2002;**106**:11354-11360. DOI: 10.1021/jp021517v

[69] Shalabi AS, El Mahdy AM, Assem MM, Taha HO, Soliman KA. Theoretical characterization of highly efficient porphyrazin dye sensitized solar cells. Journal of Nanoparticle Research. 2014;**16**:2579-2595. DOI: 10.1007/s11051-014-2579-8

[70] Lu X, Wei S, Wu CML, Li S, Guo W. Can polypyridyl Cu(I)-based complexes provide promising sensitizers for dye-sensitized solar cells? A theoretical insight into Cu(I) versus Ru(II) sensitizers. The Journal of Physical Chemistry C. 2011;**115**:3753-3761. DOI: 10.1021/jp111325y

[71] Moser J, Punchihewa S, Infelta PP, Grätzel M. Surface complexation of colloidal semiconductors strongly enhances interfacial electron-transfer rates. Langmuir. 1991;**7**:3012-3018. DOI: 10.1021/la00060a018

[72] Abuabara SG, Rego LGC, Batista VS. Influence of thermal fluctuations on interfacial electron transfer in functionalized TiO₂ semiconductors. Journal of the American Chemical Society. 2005;**127**:18234-18242. DOI: 10.1021/ja055185u

[73] Persson P, Bergström R, Lunell S. Quantum chemical study of photoinjection processes in dye-sensitized TiO₂ nanoparticles. The Journal of Physical Chemistry B. 2000;**104**:10348-10351. DOI: 10.1021/jp002550p

[74] Li SC, Wang J, Jacobson P, Gong XQ, Selloni A, Diebold U. Correlation between bonding geometry and band gap states at organic-inorganic interfaces: Catechol on rutile TiO₂(110). Journal of the American Chemical Society. 2009;**131**:980-984. DOI: 10.1021/ja803595u

[75] Oprea CI, Panait P, Cimpoesu F, Ferbinteanu M, Gîrţu MA. Density functional theory (DFT) study of coumarin-based dyes adsorbed on TiO₂ nanoclusters-applications to dye-sensitized solar cells. Materials. 2013;**6**:2372-2392. DOI: 10.3390/ma6062372

[76] De Angelis F, Fantacci S, Gebauer R. Simulating dye-sensitized TiO₂ heterointerfaces in explicit solvent: Absorption spectra, energy levels, and dye desorption. The Journal of Physical Chemistry Letters. 2011;**2**:813-817. DOI: 10.1021/jz200191u

[77] Junge H, Codolà Z, Kammer A, Rockstroh N, Karnahl M, Luo SP, et al. Copper-based water reduction catalysts for efficient light-driven hydrogen generation. Journal of Molecular Catalysis A: Chemical. 2014;**395**:449-456. DOI: 10.1016/j.molcata.2014.09.005

[78] Lee CH, Dogutan DK, Nocera DG. Hydrogen generation by Hangman metalloporphyrins. Journal of the American Chemical Society. 2011;**133**:8775-8777. DOI:10.1021/ja202136y

[79] Bhattacharjee A, Andreiadis ES, Chavarot-Kerlidou M, Fontecave M, Field MJ, Artero V. A computational study of the mechanism of hydrogen evolution by cobalt(diiminedioxime) catalysts. Chemistry–A European Journal. 2013;**19**:15166-15174. DOI: 10.1002/chem.201301860

[80] Joliat E, Schnidrig S, Probst B, Bachmann C, Spingler B, Baldridge KK, et al. Cobalt complexes of tetradentate, bipyridine-based macrocycles: Their structures, properties and photocatalytic proton reduction. Dalton Transactions. 2016;**45**:1737-1745. DOI:10.1039/C5DT04426J

[81] Guttentag M, Rodenberg A, Kopelent R, Probst B, Buchwalder C, Brandstätter M, et al. Photocatalytic H_2 production with a rhenium/cobalt system in water under acidic conditions. European Journal of Inorganic Chemistry. 2012;**2012**:59-64. DOI: 10.1002/ejic.201100883

[82] Tran PD, Wong LH, Barber J, Loo JSC. Recent advances in hybrid photocatalysts for solar fuel production. Energy and Environmental Science. 2012;**5**:5902-5918. DOI: 10.1039/C2EE02849B

[83] Fujishima A, Honda K. Electrochemical photolysis of water at a semiconductor electrode. Nature. 1972;**238**:37-38. DOI: 10.1038/238037a0

[84] Baraton MI. Nano-TiO_2 for solar cells and photocatalytic water splitting: Scientific and technological challenges for commercialization. The Open Nanoscience Journal. 2011;**5**:64-77. DOI: 10.2174/1874140101105010064

[85] Linsebigler AL, Lu G, Yates JT. Photocatalysis on TiO_2 surfaces: principles, mechanisms, and selected results. Chemical Reviews. 1995;**95**:735-758. DOI: 10.1021/cr00035a013

[86] Bard AJ, Fox MA. Artificial photosynthesis: Solar splitting of water to hydrogen and oxygen. Accounts of Chemical Research. 1995;**28**:141-145. DOI: 10.1021/ar00051a007

[87] Bikondoa O, Pang CL, Ithnin R, Muryn CA, Onishi H, Thornton G. Direct visualization of defect-mediated dissociation of water on TiO_2(110). Nature Materials. 2006;**5**:189-192. DOI: 10.1038/nmat1592

[88] Wendt S, Matthiesen J, Schaub R, Vestergaard EK, Lægsgaard E, Besenbacher F, et al. Formation and splitting of paired hydroxyl groups on reduced TiO_2(110). Physical Review Letters. 2006;**96**:66107-66110. DOI: 10.1103/PhysRevLett.96.066107

[89] Zhao ZY. Single water molecule adsorption and decomposition on the low-index stoichiometric rutile TiO_2 surfaces. The Journal of Physical Chemistry C. 2014;**118**:4287-4295. DOI: 10.1021/jp500177n

[90] Hahn KR, Tricoli A, Santarossa G, Vargas A, Baiker A. First principles analysis of H_2O adsorption on the (110) surfaces of SnO_2, TiO_2 and their solid solutions. Langmuir. 2012;**28**:1646-1656. DOI:10.1021/la204124p

[91] Monti A, de Ruiter JM, de Groot HJM, Buda F. A dynamic view of proton-coupled electron transfer in photocatalytic water splitting. The Journal of Physical Chemistry C. 2016;**120**:23074-23082. DOI: 10.1021/acs.jpcc.6b08244

[92] Hanaor DAH, Assadi MHN, Li S, Yu A, Sorrell CC. Ab initio study of phase stability in doped TiO2. Computational Mechanics. 2012;**50**:185-194. DOI: 10.1007/s00466-012-0728-4

[93] Zhang Y, Kilin DS. Computational modeling of wet TiO$_2$ (001) anatase surfaces functionalized by transition metal doping. International Journal of Quantum Chemistry. 2012;**112**:3867-3873. DOI: 10.1002/qua.24289

[94] Zhang ST, Li CM, Yan H, Wei M, Evans DG, Duan X. Density functional theory study on the metal-support interaction between Ru cluster and anatase TiO$_2$(101) surface. The Journal of Physical Chemistry C. 2014;**118**:3514-3522. DOI:10.1021/jp409627p

[95] Graciani J, Plata JJ, Sanz JF, Liu P, Rodriguez JA. A theoretical insight into the catalytic effect of a mixed-metal oxide at the nanometer level: The case of the highly active metal/CeO$_x$/TiO$_2$(110) catalysts. The Journal of Chemical Physics. 2010;**132**:104703-104710. DOI: 10.1063/1.3337918

[96] Pastore M, De Angelis F. First-principles modeling of a dye-sensitized TiO$_2$/IrO$_2$ photoanode for water oxidation. Journal of the American Chemical Society. 2015;**137**:5798-5809. DOI: 10.1021/jacs.5b02128

[97] Harris LA, Quong AA. Molecular chemisorption as the theoretically preferred pathway for water adsorption on ideal rutile TiO$_2$(110). Physical Review Letters. 2004;**93**:086105-086108. DOI: 10.1103/PhysRevLett.93.086105

[98] Wilhelm J, Seewald P, Del Ben M, Hutter J. Large-scale cubic-scaling random phase approximation correlation energy calculations using a Gaussian basis. Journal of Chemical Theory and Computation. 2016;**12**:5851-5859. DOI:10.1021/acs.jctc.6b00840

[99] Xu H, Zhang RQ, Ng AMC, Djurišić AB, Chan HT, Chan WK, et al. Splitting water on metal oxide surfaces. The Journal of Physical Chemistry C. 2011;**115**:19710-19715. DOI:10.1021/jp2032884